

Research Articles | Development/Plasticity/Repair

## Mapping early brain-body interactions: associations of fetal heart rate variation with newborn brainstem, hypothalamic, and dorsal anterior cingulate cortex functional connectivity

<https://doi.org/10.1523/JNEUROSCI.2363-23.2024>

Received: 15 December 2023

Revised: 31 March 2024

Accepted: 3 April 2024

Copyright © 2024 the authors

---

*This Early Release article has been peer reviewed and accepted, but has not been through the composition and copyediting processes. The final version may differ slightly in style or formatting and will contain links to any extended data.*

**Alerts:** Sign up at [www.jneurosci.org/alerts](http://www.jneurosci.org/alerts) to receive customized email alerts when the fully formatted version of this article is published.

1 **Title: Mapping early brain-body interactions: associations of fetal heart rate variation**  
2 **with newborn brainstem, hypothalamic, and dorsal anterior cingulate cortex functional**  
3 **connectivity**

4 **Abbreviated title: Fetal heart rate and newborn brain associations**

5 Authors: Angeliki Pollatou<sup>1</sup>, Cristin M. Holland<sup>1</sup>, Thirsten J. Stockton<sup>1</sup>, Bradley S. Peterson<sup>2,3</sup>,  
6 Dustin Scheinost<sup>4,5,6,7,8\*</sup>, Catherine Monk<sup>1,9\*</sup>, Marisa N. Spann<sup>1\*</sup>

7 Affiliations:

8 <sup>1</sup>Department of Psychiatry, Columbia University Vagelos College of Physicians and Surgeons,  
9 New York, NY 10032

10 <sup>2</sup>Institute for the Developing Mind, Children's Hospital Los Angeles, Los Angeles, CA 90027

11 <sup>3</sup>Department of Psychiatry, Keck School of Medicine, University of Southern California, Los  
12 Angeles, CA 90033

13 <sup>4</sup>Departments of Radiology and Biomedical Imaging, Yale School of Medicine, New Haven, CT  
14 06520

15 <sup>5</sup>Child Study Center, Yale School of Medicine, New Haven, CT 06520

16 <sup>6</sup>Department of Biomedical Engineering, Yale School of Engineering and Applied Science, New  
17 Haven, CT 06520

18 <sup>7</sup>Department of Statistics and Data Science, Yale University, New Haven, CT 06511

19 <sup>8</sup>Wu Tsai Institute, Yale University, New Haven, CT 06506

20 <sup>9</sup>Department of Obstetrics and Gynecology, Vagelos College of Physicians and Surgeons,  
21 Columbia University 10032

22

23 \*indicates shared senior authorship

24

25 **Corresponding Author:**

26 Marisa N. Spann, PhD, MPH

27 Columbia University Irving Medical Center

28 622 West 168<sup>th</sup> Street, PH Room 1540

29 New York, NY 10032

30 Email: mns2125@cumc.columbia.edu

31 Phone: (646) 774-5824

32

33 **Number of pages: 16 pages (text, without references), 8 pages (tables and figures)**

34 **Number of figures, tables, multimedia, and 3D models (separately): 2 tables, 6 figures**

35 **Number of words for abstract, introduction and discussion (separately): 231, 664, 1091**

36

37

38  
39  
40  
41  
42  
43  
44  
45  
46  
47  
48  
49  
50  
51  
52  
53

### **Conflict of Interest Statement**

The authors declare no competing financial interests.

### **Acknowledgments**

This work was supported by the National Institute of Mental Health (NIMH) R01MH093677 (C.M. & B.S.P.), the Eunice Kennedy Shriver National Institute for Child Health and Human Development K23HD092589 (M.S.), the NIMH K24MH127381 (M.S.) and R01MH126133 (M.S. & D.S.), and the National Center for Advancing Translational Sciences TL1TR001875 (A.P. & C.H.) grants. We would like to thank Kristiana Barbato, Alida Davis, Erica Lambeth, and Ashley Rainford for their support with data collection and Grace Liu for her support with data management. The content is solely the responsibility of the authors and does not necessarily represent the official views of the NIH.

**Keywords:** autonomic nervous system, heart rate, heart rate variability, infant, brain, fMRI, HR, HRV, hypothalamus, brainstem, dACC, language, memory, motor control

54

## Abstract

55       The autonomic nervous system (ANS) regulates the body's physiology, including  
56 cardiovascular function. As the ANS develops during the second to third trimester, fetal heart rate  
57 variability (HRV) increases while fetal heart rate (HR) decreases. In this way, fetal HR and HRV  
58 provide an index of fetal autonomic nervous system development and future neurobehavioral  
59 regulation. Fetal HR and HRV have been associated with child language ability and psychomotor  
60 development behavior in toddlerhood. However, their associations with post-birth autonomic brain  
61 systems, such as the brainstem, hypothalamus, and dorsal anterior cingulate cortex (dACC), have  
62 yet to be investigated even though brain pathways involved in autonomic regulation are well  
63 established in older individuals. We assessed whether fetal HR and HRV were associated with  
64 the brainstem, hypothalamic and dACC functional connectivity in newborns. Data were obtained  
65 from 60 pregnant individuals (ages 14-42) at 24-27 and 34-37 weeks gestation using a fetal  
66 actocardiograph to generate fetal HR and HRV. During natural sleep, their infants (38 males and  
67 22 females) underwent a fMRI scan between 40-46 weeks of postmenstrual age. Our findings  
68 relate fetal heart indices to brainstem, hypothalamic, and dACC connectivity and reveal  
69 connections with widespread brain regions that may support behavioral and emotional regulation.  
70 We demonstrated the basic physiologic association between fetal HR indices and lower and  
71 higher order brain regions involved in regulatory processes. This work provides the foundation for  
72 future behavioral or physiological regulation research in fetuses and infants.

73

74

75

76

77

78

79

### **Significance statement**

80 Fetal heart rate indices are quantifiable, developmental markers of the fetal autonomic nervous  
81 system. Variations in their trajectories can signal compromised neurodevelopmental outcomes.  
82 We assessed associations between fetal heart rate indices and early infant brain development to  
83 identify unique or common associations corresponding to autonomic nervous system maturation  
84 patterns. We found associations between fetal heart rate indices and infant brainstem,  
85 hypothalamic, and dACC connectivity—areas that support autonomic and behavioral regulatory  
86 functions. The study demonstrates that these associations between ANS and brain regions  
87 involved in autonomic regulation exist early in life. These findings are a first step to understanding  
88 how these brain connections form the basis of future regulatory development.

89

90

91

JNeurosci Accepted Manuscript

## 1. Introduction

93 The autonomic nervous system (ANS) is a component of the peripheral nervous system  
94 that regulates the body's physiology. It cooperatively modulates the heart rate through the  
95 sympathetic nervous system (SNS) and the parasympathetic nervous system (PNS). The brain  
96 pathways involved in autonomic regulation are well-established in human adults. For example,  
97 the hypothalamus connects the lower-order (including the medulla oblongata) and higher-order  
98 (including the dorsal anterior cingulate—dACC) nervous systems to interpret environmental  
99 stimuli and regulate cardiovascular function (Ulrich-Lai and Herman, 2009).

100 The ANS regulatory capacity begins as early as eight weeks gestation. ANS activity is a  
101 marker of developing fetal brain functions and modulates cardiovascular responses (David et al.,  
102 2007; Chouchou and Desseilles, 2014). Fetal ANS development can be non-invasively assessed  
103 with fetal heart rate (HR) and fetal heart rate variability (HRV) (Spann et al., 2014; Spann et al.,  
104 2015; de la Cruz et al., 2019). Internal and external stimuli cause autonomic adjustments to  
105 maintain homeostasis, resulting in natural HR and HRV variations (Oliveira et al., 2019). Fetal HR  
106 is mainly controlled by the SNS early in gestation and the PNS later in gestation (Hofmeyr et al.,  
107 2014). During the transition from the late second into the third trimester, the development of fetal  
108 HR is driven by the increase of the parasympathetic influence and the changes in autonomic  
109 control from the medulla to higher cortical regions (David et al., 2007; DiPietro et al., 2015). This  
110 shift is reflected in the decline of mean fetal HR during rest (DiPietro et al., 2001; DiPietro et al.,  
111 2015; Heuser, 2020; Cerritelli et al., 2021). By 30 weeks gestation, ANS modulation involves input  
112 from the dACC and medial prefrontal cortex (mPFC) (Robinson et al., 1966; Horiuchi et al., 2006).

113 Fetal HR and HRV are also associated with risk for poor neurodevelopmental outcomes  
114 (Hofmeyr et al., 2014; Karmakar et al., 2015; Howland et al., 2020). Fetal HR and HRV correlate  
115 with later higher motor control and language development scores (DiPietro et al., 2007) and early  
116 temperament and emotion regulation scores (Feldman, 2006; Werner et al., 2007; DiPietro et al.,

117 2018; Howland et al., 2020; Pingeton et al., 2021). Additionally, prenatal exposures to maternal  
118 hyperglycemia and environmental toxins can alter fetal ANS development (DiPietro et al., 1999;  
119 Monk et al., 2000; DiPietro et al., 2002; Monk et al., 2004; Zisser et al., 2006; DiPietro et al.,  
120 2013). Overall, this suggests fetal ANS activity, as measured by HR indices, is an important  
121 indicator for developmental outcomes.

122 Functional neuroimaging studies with healthy adults connect cortico-limbic activity and  
123 autonomic regulation (de la Cruz et al., 2019). Strong age-dependent associations exist between  
124 HRV and functional connectivity of the posterior cingulate cortex and the medial prefrontal cortex  
125 (mPFC) (Kumral et al., 2019). Connectivity between brain regions involved in ANS regulation  
126 exists as early as 24-27 weeks of gestation (Thomason et al., 2015; Borsani et al., 2019). Further,  
127 functional networks are largely observable in the neonatal period (Doria et al., 2010; Gao et al.,  
128 2015; Gao et al., 2017). For example, dACC shows strong connectivity to the insula in the  
129 neonatal period (Spann et al., 2018). Nevertheless, studies associating early brain functioning  
130 with ANS regulation are lacking. In the single published study, higher fetal HRV assessed at 34–  
131 37 weeks gestation was positively associated with greater infant connectivity between the dACC  
132 and mPFC (Spann et al., 2018).

133 This study investigated the associations between fetal HR indices during the second and  
134 third trimesters and newborn brain connectivity. We acquired fetal HR data during the second and  
135 third trimesters to measure fetal ANS development. We assessed brainstem, hypothalamus, and  
136 dACC functional connectivity using resting-state fMRI data acquired at 40-46 weeks  
137 postmenstrual age (PMA). Our primary hypothesis was that third trimester fetal HR indices would  
138 associate significantly with newborn functional brain connectivity in the seed areas involved with  
139 the ANS. Our secondary hypothesis was that second trimester fetal HR and HRV would yield  
140 similar associations. The novelty of this research precluded specific hypotheses about the  
141 direction of these effects.

143  
144  
145  
146  
147  
148  
149  
150  
151  
152  
153  
154  
155  
156  
157  
158  
159  
160  
161  
162  
163  
164  
165  
166

## 2. Materials and Methods

### 2.1. Participants

Pregnant individuals, aged 14-42, were recruited in the second trimester (13-28 weeks) through the Departments of Obstetrics and Gynecology at Columbia University Irving Medical Center (CUIMC), Weill Cornell Medical College, and flyers posted in the CUIMC vicinity. All pregnant participants had no major health problems during recruitment and received routine prenatal care. Adult participants provided informed consent. If they were under 18, they completed an assent form, and their parent signed a consent form. The New York State Psychiatric Institute Institutional Review Board approved the procedures. Participants were excluded from the studies if they acknowledged using recreational drugs, tobacco, or alcohol, taking medications that affect cardiovascular function, or not speaking English fluently.

### 2.2. Fetal assessment

To maximize reproducibility, pregnant individuals participated in a standardized, validated protocol (Besinger and Johnson, 1989; DiPietro et al., 1999; DiPietro et al., 2004). They were asked to refrain from eating 1.5 hours before the visit. During data collection, individuals were awake to avoid acute increases or decreases in fetal HR or movement that would affect data collection. Finally, HR indices were collected after 20 weeks of gestation when they are more stable.

Fetal HR was acquired while the participants were in a semi-recumbent position for 20 minutes, using a Toitu MT 325 fetal actocardiograph (Toitu Co.,Ltd, Tokyo, Japan) during the 24-27<sup>th</sup> (second trimester) and 34-37<sup>th</sup> (third trimester) weeks of gestation. The Toitu detects fetal HR via a single transabdominal Doppler transducer. The signal is processed through a series of filters. These filters remove the frequency components of the Doppler signal that are associated with fetal HR (Besinger and Johnson, 1989; DiPietro et al., 1999; DiPietro et al., 2004). Fetal HR output



167 was digitized at 50 Hz using a 16 bit A/D card (National Instruments 16XE50). Fetal HR below 80  
168 beats per minute (bpm) or above 200 bpm were removed. Custom MATLAB programs  
169 (<http://www.mathworks.com>) were used to calculate mean fetal HR and the standard deviation of  
170 fetal HR (i.e., HRV). A detailed algorithm description has previously been published (Doyle et al.,  
171 2015; Spann et al., 2015; Spann et al., 2018).

## 172 2.3. Infant imaging

### 173 2.3.1 Infant MRI preparation and data acquisition

174 Sixty infants (38 males and 22 females) were scanned within the first weeks of  
175 postmenstrual life (PMA  $\leq$  46 weeks). After they were fed and swaddled, they were given time to  
176 fall asleep naturally. We used foam ear plugs, wax, and ear shields (Natus Medical) to dampen  
177 the scanner noise. The infants' heart rate and oxygen saturation were monitored continually  
178 during the scan (InVivo Research, Biopac). Images were obtained using a 3 Tesla Signa MRI  
179 scanner (General Electric).

180 There are two different sets of parameters using during scanning, earlier subjects used a  
181 different sequence than the later subjects. The images for the earlier subjects (n=38) were  
182 acquired using a 3 Tesla General Electric Signa MRI scanner with an eight-channel head coil. A  
183 2D, multiple shot, fast spin echo sequence was employed to obtain high-resolution anatomical  
184 T2-weighted images, with PROPELLER (Periodically Rotated Overlapping Parallel Lines with  
185 Enhanced Reconstruction) used to decrease motion artifacts in the reconstructed MR images  
186 (Pipe, 1999): repetition time (TR) = 10,000 ms; echo time (TE) = 130 ms; echo train length (ETL)  
187 = 32; matrix size = 192  $\times$  192; field of view (FOV) = 190  $\times$  190 mm; phase FOV = 100%; slice  
188 thickness = 1.0 mm; number of excitations (NEX) = 2. The spatial resolution of the T2-weighted  
189 images was 1 mm<sup>3</sup>. Functional images were acquired using a standard echoplanar imaging  
190 sequence: TR = 2200 ms; TE = 30 ms; matrix size = 64  $\times$  64; FOV = 190  $\times$  190 mm; phase FOV

191 = 100%; slice thickness = 5.0 mm, contiguous; number of slices = 24; bandwidth = 7812.5 Hz;  
192 voxel size = 2.969 x 2.969 x 5. Due to the infant waking, the number of runs acquired were  
193 different for each participant. A median of 6 runs of 102 volumes (3 min 44.4s each) were collected  
194 per infant. The images for the newer subjects (n=10) were acquired using a 3 Tesla General  
195 Electric Signa Premier with a 48-channel head coil and the anatomical T2-weighted images were  
196 acquired with: TR=3202 ms; TE=60 ms; matrix size=256x256; FOV=256x256 mm; phase  
197 FOV=100%; ETL=140; slice thickness=0.9 mm. Functional images for the new subjects were  
198 acquired using a standard echoplanar imaging sequence: TR=2000 ms; TE=30 ms; matrix  
199 size=64 x 64; FOV=190 x 190 mm; phase FOV = 100%; slice thickness = 3.0mm; number of  
200 slices = 34; bandwidth=7812.5 Hz; voxel size = 2.969 x 2.969 x 3. The functional sequences have  
201 built-in discarded volumes to allow the tissue to reach a steady state. The number of runs varied  
202 per participant and a median of 3 runs of 90 volumes were obtained for each infant. When  
203 combining all participants, we removed the last 12 volumes from the fMRI data from the earlier  
204 subjects to match the number of volumes from the newer subjects.

### 205 2.3.2. *Pre-processing*

206 Anatomical images were skull stripped using FSL (<https://fsl.fmrib.ox.ac.uk/fsl/>). If, after  
207 visual inspection, any non-brain tissue remained, it was removed manually. Unless otherwise  
208 specified, all further analyses were performed using BiImage Suite (Joshi et al., 2011).  
209 Anatomical images were non-linear registered to a custom, age-appropriate template (Spann et  
210 al., 2018) using a validated algorithm (Scheinost et al., 2017). After the anatomical scans were  
211 registered to the template, functional images were rigidly aligned to the anatomical images. All  
212 transformation pairs were calculated independently and combined into a single transform, warping  
213 the single participant results into common space. This single transformation allows the individual  
214 participant images to be transformed to common space with only one transformation, thereby  
215 reducing interpolation error.

216 We performed motion correction on the functional data with SPM12  
217 (<https://www.fil.ion.ucl.ac.uk/spm/>). The frame-to-frame motion was calculated across all the  
218 functional volumes. Data were further cleaned as previously described (Kwon et al., 2014). Linear  
219 and quadratic drifts, mean cerebrospinal fluid signal, mean white matter signal, mean gray matter  
220 signal, and a 24-parameter motion model (6 motion parameters, 6 temporal derivatives, and their  
221 squares) were regressed from the data. A Gaussian filter with an approximate cutoff frequency of  
222 0.12 Hz was used to smooth the functional data temporarily.

223 Because motion and the amount of data available for analysis can affect functional  
224 connectivity measures (Van Dijk et al., 2012; Noble et al., 2017), we used a strict inclusion  
225 criterion that participants had at least 2 runs of data with an average frame-to-frame motion of  
226 <0.15 mm. We used the average of 2 runs per subject. Only one infant was removed using these  
227 criteria. If more than two resting state runs were available, we included the ones with the lowest  
228 average frame-to-frame motion in the analysis.

### 229 2.3.3. Seed connectivity

230 The seed regions of interest were defined as the bilateral medulla, hypothalamus, and  
231 dorsal anterior cingulate cortex (dACC). The seeds were manually defined on the reference brain  
232 (Fig. 1). The approximate MNI coordinates are: dACC (-1,24,26), medulla (-4,-36,-35), and  
233 hypothalamus (-2,-3,-3). The temporal signal noise ratios for each seed are  $170.71 \pm 109.35$  for  
234 the dACC,  $49.37 \pm 32.84$  for the medulla, and  $65.36 \pm 34.86$  for the hypothalamus. In each  
235 participant, the time course of the reference region was computed by averaging the time course  
236 of every voxel within the seed region. This time course was correlated with the time course for  
237 every voxel in gray matter to create a map of r-values representing seed-to-whole-brain  
238 connectivity. Using the Fisher's transform, we transformed these r-values to z-values, generating  
239 one map for each seed and representing the strength of correlation with the seed for each  
240 participant.

241 *2.4. Statistical analyses*

242 Our primary analysis assessed the association of mean resting fetal HR and HRV during  
243 the third trimester with measures of connectivity of the seed areas to the whole brain. The second-  
244 trimester associations were also assessed. Our sample during the second trimester was smaller  
245 (n=33) than in the third trimester (n=48); therefore, these results are presented as secondary.  
246 Finally, for exploratory analyses, we associated the change from second to third trimester fetal  
247 HR indices and seed connectivity (n=27). The imaging data were analyzed using voxel-wise linear  
248 models controlling for biological sex, motion, maternal age, scanner/sequence, and PMA.  
249 Significant imaging clusters were shown at  $p < 0.05$ , corrected for multiple statistical comparisons.  
250 We corrected for multiple comparisons across gray matter using cluster-level correction estimated  
251 via AFNI's 3dClustSim (version 16.3.05, <https://afni.nimh.nih.gov/>) with 10,000 iterations,  
252 smoothness estimated with the -ACF option, an initial cluster forming threshold of  $p = 0.001$ , and  
253 the gray matter mask applied in preprocessing.

254

255

### 3. Results

#### 3.1. Demographics

257 Of the 60 participants, our final sample size consisted of 48 neonates with usable fetal HR  
258 in the third trimesters and high-quality fMRI data and of 33 neonates with usable fetal HR in the  
259 second trimesters and high-quality fMRI data. The average age of the pregnant women was 21  
260 ( $20.98 \pm 5.5$ ) years; the majority were Hispanic (80%). Neonates were scanned at an average 43  
261 ( $42.97 \pm 2.04$ ) weeks PMA; the majority were male (63%). The infants were healthy and were  
262 born without delivery complications at gestational age  $>37$  weeks. The mean frame-to-frame  
263 motion was 0.05 mm and was not correlated with our main outcomes (fetal HR and HRV;  
264  $r$ 's $<0.05$ ).

#### 3.2. Primary Analyses

266 *3.2.1. Associations of mean resting fetal HR in the third trimester with bilateral medulla, dACC,  
267 and hypothalamic connectivity in neonates (n=48).*

268 Higher mean fetal HR was positively associated with the connectivity between the medulla  
269 and the bilateral precentral and postcentral gyrus and the right inferior parietal lobe (IPL; Fig. 2).  
270 Higher mean fetal HR displayed a positive association with the connectivity between the  
271 hypothalamus and the left and right anterior part of the middle frontal gyrus (MFG) (Fig. 2). Higher  
272 mean fetal HR was inversely associated with connectivity between the dACC and left cerebellum.  
273 Additionally, higher mean fetal HR was associated with positive connectivity between the dACC  
274 and a cluster that extends in the IPL and the superior temporal gyrus (STG; Fig. 2). The location  
275 and size of all significant clusters are summarized in Table 1.

276 *3.2.2. Associations of fetal HRV in the third trimester with bilateral medulla, dACC, and  
277 hypothalamic connectivity in neonates (n=48).*

278 Higher fetal HRV was positively associated with the connectivity between the medulla and  
279 the left precuneus and paracentral lobule (Fig. 3). Higher fetal HRV was inversely associated with  
280 the connectivity between the hypothalamus and the left middle temporal gyrus (Fig. 3). Higher  
281 fetal HRV was positively associated with connectivity between the bilateral dACC and the left  
282 superior frontal gyrus and between the bilateral dACC and the right lateral occipital gyrus (Fig. 3).  
283 The location and size of all significant clusters are summarized in Table 1.

### 284 **3.3. Secondary analyses**

285 *3.3.1. Associations of mean resting fetal HR in the second trimester with bilateral medulla,*  
286 *hypothalamic, and dACC connectivity in neonates (n=33).*

287 Higher mean fetal HR was inversely associated with the medulla-left MFG connectivity  
288 and positively with medulla-right STG and IPL connectivity (Fig. 4). Higher mean fetal HR was  
289 positively associated with the connectivity between the hypothalamus and left subcortex and  
290 between the hypothalamus and left precuneus/paracentral lobule (Fig. 4). Higher mean fetal HR  
291 was inversely associated with the connectivity between the dACC and the right cerebellum,  
292 between the dACC and the right basal ganglia, and between the dACC and left insula (Fig. 4).  
293 Higher mean fetal HR was associated with the connectivity between the dACC and the bilateral  
294 visual cortex and between the dACC and the right lateral occipital gyrus (Fig. 4). The location and  
295 size of all significant clusters are summarized in Table 2.

296 *3.3.2. Associations of fetal HRV in the second trimester with bilateral medulla, hypothalamic, and*  
297 *dACC connectivity in neonates (n=33).*

298 Higher fetal HRV was positively associated with the connectivity between the medulla and  
299 right cerebellum, between the medulla and the left fusiform gyrus/cerebellum, and between the  
300 medulla and right SPL (Fig. 5). Higher fetal HRV was positively associated with connectivity  
301 between hypothalamus and right and left subcortex (Fig. 5). Higher fetal HRV was positively

302 associated with connectivity between dACC and middle cingulate cortex (Fig. 5). The location and  
303 size of all significant clusters are summarized in Table 2.

### 304 **3.4. Exploratory analyses**

305 *3.4.1. Associations of the change in mean fetal HR from the second to third trimester with bilateral*  
306 *medulla, hypothalamic, and dACC connectivity in newborns (n=27).*

307 Higher change in fetal HR was positively associated with the connectivity between the  
308 medulla and the left precentral and postcentral gyrus (Fig. 6). Higher change in fetal HR was  
309 inversely associated with the connectivity between the medulla and the cerebellum (Fig. 6). No  
310 associations with the hypothalamus were observed. Higher change in fetal HR was positively  
311 associated with the connectivity between the dACC and the right inferior frontal gyrus (Fig. 6).  
312 The location and size of all significant clusters are summarized in Table 3.

313 *3.4.2. Associations of the change in fetal HRV from the second to third trimester with bilateral*  
314 *medulla, hypothalamic, and dACC connectivity in neonates (n=27).*

315 Higher change in fetal HRV was positively associated with the connectivity between the  
316 medulla and the right inferior occipital gyrus (Fig. 7). Higher change in fetal HRV was inversely  
317 associated with the connectivity between the medulla and the left hippocampus and between the  
318 medulla and the right cerebellum (Fig. 7). Higher change in fetal HRV was positively associated  
319 with the connectivity between the hypothalamus and the bilateral precuneus and paracentral  
320 lobule and between the hypothalamus and the left precentral gyrus (Fig. 7). Higher change in fetal  
321 HRV was inversely associated with the connectivity between the hypothalamus and left middle  
322 temporal gyrus (Fig. 7). Higher change in fetal HRV was positively associated with the connectivity  
323 between the dACC and the left middle frontal gyrus (Fig. 7). The location and size of all significant  
324 clusters are summarized in Table 3.

325

326

327

#### 4. Discussion

328 This study investigated the associations between fetal HR indices and functional  
329 connectivity of brain regions involved in autonomic regulation, including the medulla,  
330 hypothalamus, and dACC (Critchley et al., 2003). Our main findings are significant associations  
331 ( $p < 0.05$ , corrected) within both trimesters for fetal HR and HRV with these brain regions. Our  
332 results suggest that a diverse network of brain regions engage with core regulatory regions and  
333 are thereby associated with autonomic regulation at this early age. They complement results from  
334 prior neuroimaging studies with adults, which demonstrated that multiple, widespread brain  
335 regions extending from the neocortex to the brainstem are involved in ANS regulation (Ulrich-Lai  
336 and Herman, 2009; Beissner et al., 2013; Macey et al., 2015; de la Cruz et al., 2019; Matusik et  
337 al., 2023).

338 Though links have been shown in non-human primates and adults (Candia-Rivera, 2022),  
339 this study demonstrates that these associations between ANS and brain regions involved in  
340 autonomic regulation exist early in life. These findings align with the maturation of autonomic  
341 regulation. The medulla oblongata is a primary regulator of fetal heart rate, but autonomic  
342 regulation shifts to include higher-order cortical regions around the end of the second trimester  
343 (Jongen et al., 2017; Mulkey and Plessis, 2018; Heuser, 2020). For example, ANS regulation  
344 involves input from the dACC and mPFC by 30 weeks gestation, which is characterized by a  
345 decline in mean fetal HR during rest (Robinson et al., 1966; DiPietro et al., 2001; Horiuchi et al.,  
346 2006; DiPietro et al., 2015; Heuser, 2020; Cerritelli et al., 2021). This progression is reflected in  
347 our fetal HR findings. For example, in our exploratory analyses, positive associations are  
348 observed in cortical areas, whereas inverse associations are observed in the subcortex and  
349 cerebellum, consistent with the shift to higher-order cortical regions in the third trimester.



350 Our findings aid the understanding of the ANS in behavioral and emotional regulation, as  
351 well. These functions are important in identifying risks for compromised development of self-  
352 regulation. Indeed, the motivation and ability to regulate internal physiological states serve as a  
353 foundation for other social-emotional regulation (Thompson and Levitt, 2010). Fetal HR and HRV  
354 associated with brain regions involved in behavioral and emotional regulation in early infancy. For  
355 example, the post-central gyrus, hypothalamus, and temporal lobe play roles in sensory and  
356 emotion processing (Fanselow and Dong, 2010; Potegal, 2012; Wong and Gallate, 2012; Kropf  
357 et al., 2019). The cerebellum also plays a critical role in social and emotional functions during  
358 infancy (Koziol et al., 2014; Beuriat et al., 2022). The cerebellum and the pre- and post-central  
359 gyrus modulate various sensory and motor functions that promote appropriate infant regulation to  
360 facilitate learning and environmental engagement (Diamond, 2000; Williams et al., 2020). Sensory  
361 or emotional stimuli influence ANS regulation and higher-order brain regions involved in  
362 behavioral and emotional regulation. Fetal HR indices correlate with behavioral (DiPietro et al.,  
363 2018; Howland et al., 2020) and emotional regulation in infancy (Feldman, 2006; Pingeton et al.,  
364 2021) and sensorimotor development at two years (DiPietro et al., 2007). This study adds to the  
365 previous literature by showing that the brain correlates of ANS regulation measured during the  
366 fetal period align with previous findings.

367 Fetal HR and HRV are markers of neurodevelopmental outcomes (Hofmeyr et al., 2014;  
368 Karmakar et al., 2015; Howland et al., 2020). Prior work demonstrated their associations with  
369 motor control, language development (DiPietro et al., 2007), and temperament (Feldman, 2006;  
370 Werner et al., 2007; DiPietro et al., 2018; Howland et al., 2020; Pingeton et al., 2021). Many brain  
371 regions connected to the regulatory seed regions detected in our analyses involve similar abilities  
372 (e.g., language, speech, sensory and motor processing). For example, the strong associations  
373 between fetal HR and HRV and connectivity between language processing regions are also novel  
374 including the superior temporal and precentral gyri. Evidence has suggested that language

375 networks are already present during the third trimester of gestation (Ghio et al., 2021; Scheinost  
376 et al., 2022). There are also indications that infants are ready to learn language from birth (Berent  
377 et al., 2021). Fetal HR and HRV correlated with language ability at 2.5 years of age (DiPietro et  
378 al., 2007). However, the mechanistic link between fetal HR indices and developmental outcomes  
379 is unknown. Functional connectivity in the neonatal period may represent such a mediating  
380 pathway. Neonatal connectivity predicts short (Scheinost et al., 2020) and long-term behavioral  
381 outcomes (Sun et al., 2023). Fetal MR indices likely influence neonatal connectivity, which in turn,  
382 influence later behavior. Nevertheless, this indirect mediation path has yet to be tested and  
383 remains future research.

384         There are several strengths to this study. We acquired data prospectively beginning in the  
385 second trimester of pregnancy and continuing into infancy. Including both trimesters is a strength  
386 as it allows us to track changes in fetal HR indices and their associations with infant brain networks  
387 across pregnancy rather than provide a snapshot of one timepoint. Our study also has several  
388 limitations. Two of the three seeds used in these analyses are subcortical and brainstem  
389 structures. These seeds had lower temporal signal noise ratios (tSNR) than the dACC seed  
390 (Figure 1). The sample size is small at n=48. However, this size is consistent with other infant  
391 studies (Korom et al., 2021) and neuroimaging studies more broadly (Szucs and Ioannidis, 2020).  
392 Our data did not facilitate time course analyses. Richer indices of heart variability may show  
393 different associations than we observed. Our maternal sample was young (mean age of 21). Thus,  
394 the observed associations may not generalize to other pregnant populations. Similarly, a majority  
395 of the sample is male. Investigations into the role of sex in the current study necessitate a larger  
396 sample size for greater statistical power. Despite the longitudinal nature of our study, we did not  
397 collect neuroimaging and heart rate data simultaneously. Relatedly, we also did not have  
398 longitudinal neuroimaging data. Future work should include fetal fMRI collected at the same  
399 gestational age as the heart rate data. Further, longitudinal studies should include data on the  
400 perinatal transition to understand how birth changes any observed associations (Scheinost et al.,

401 2022). Additionally, we did not collect behavioral data during the neonatal period to correlate with  
402 the connectivity measures. The role of the observed results and later behavior is unclear. Finally,  
403 while we used a standardized protocol to minimize external influences on fetal vigilance state, the  
404 fetal vigilance state (Suwanrath and Suntharasaj, 2010) is unknown. State differences could have  
405 affected the heart rate indices. However, such discrimination of states would be challenging  
406 before 32 weeks of gestation when only periods of fetal activity and quiescence can be  
407 distinguished (Brändle et al., 2015).

## 408 **5. Conclusion**

409 Our findings show that neonatal brain regions—involved in autonomic regulation during  
410 postnatal development—have significant associations with fetal HR and HRV during the second  
411 and third trimester of gestation. They add to adult studies linking functional neuroimaging to  
412 autonomic regulation by showing association earlier in life. Future studies should aim to  
413 investigate how these brain connections mediate future development of autonomic and behavioral  
414 regulation abilities in childhood.

415

416

## References

- 417  
418  
419 Beissner F, Meissner K, Bär KJ, Napadow V (2013) The autonomic brain: an activation  
420 likelihood estimation meta-analysis for central processing of autonomic function. *J*  
421 *Neurosci* 33:10503-10511.
- 422 Berent I, de la Cruz-Pavía I, Brentari D, Gervain J (2021) Infants differentially extract rules from  
423 language. *Sci Rep* 11:20001.
- 424 Besinger RE, Johnson TR (1989) Doppler recording of fetal movement: clinical correlation with  
425 real-time ultrasound. *Obstet Gynecol* 74:277-280.
- 426 Beuriat PA, Cristofori I, Gordon B, Grafman J (2022) The shifting role of the cerebellum in  
427 executive, emotional and social processing across the lifespan. *Behav Brain Funct* 18:6.
- 428 Borsani E, Della Vedova AM, Rezzani R, Rodella LF, Cristini C (2019) Correlation between  
429 human nervous system development and acquisition of fetal skills: An overview. *Brain*  
430 *Dev* 41:225-233.
- 431 Brändle J, Preissl H, Draganova R, Ortiz E, Kagan KO, Abele H, Brucker SY, Kiefer-Schmidt I  
432 (2015) Heart rate variability parameters and fetal movement complement fetal behavioral  
433 states detection via magnetography to monitor neurovegetative development. *Front Hum*  
434 *Neurosci* 9:147.
- 435 Candia-Rivera D (2022) Brain-heart interactions in the neurobiology of consciousness. *Curr Res*  
436 *Neurobiol* 3:100050.
- 437 Cerritelli F, Frasch MG, Antonelli MC, Viglione C, Vecchi S, Chiera M, Manzotti A (2021) A  
438 Review on the Vagus Nerve and Autonomic Nervous System During Fetal Development:  
439 Searching for Critical Windows. *Front Neurosci* 15:721605.
- 440 Chouchou F, Desseilles M (2014) Heart rate variability: a tool to explore the sleeping brain?  
441 *Front Neurosci* 8:402.
- 442 Critchley HD, Mathias CJ, Josephs O, O'Doherty J, Zanini S, Dewar BK, Cipolotti L, Shallice T,  
443 Dolan RJ (2003) Human cingulate cortex and autonomic control: converging  
444 neuroimaging and clinical evidence. *Brain* 126:2139-2152.
- 445 David M, Hirsch M, Karin J, Toledo E, Akselrod S (2007) An estimate of fetal autonomic state by  
446 time-frequency analysis of fetal heart rate variability. *J Appl Physiol* (1985) 102:1057-  
447 1064.
- 448 de la Cruz F, Schumann A, Köhler S, Reichenbach JR, Wagner G, Bär KJ (2019) The  
449 relationship between heart rate and functional connectivity of brain regions involved in  
450 autonomic control. *Neuroimage* 196:318-328.
- 451 Diamond A (2000) Close interrelation of motor development and cognitive development and of  
452 the cerebellum and prefrontal cortex. *Child Dev* 71:44-56.
- 453 DiPietro JA, Costigan KA, Pressman EK (1999) Fetal movement detection: comparison of the  
454 Toitu actograph with ultrasound from 20 weeks gestation. *J Matern Fetal Med* 8:237-  
455 242.
- 456 DiPietro JA, Costigan KA, Voegtline KM (2015) STUDIES IN FETAL BEHAVIOR: REVISITED,  
457 RENEWED, AND REIMAGINED. *Monogr Soc Res Child Dev* 80:vii;1-94.
- 458 DiPietro JA, Voegtline KM, Pater HA, Costigan KA (2018) Predicting child temperament and  
459 behavior from the fetus. *Dev Psychopathol* 30:855-870.
- 460 DiPietro JA, Irizarry RA, Hawkins M, Costigan KA, Pressman EK (2001) Cross-correlation of  
461 fetal cardiac and somatic activity as an indicator of antenatal neural development. *Am J*  
462 *Obstet Gynecol* 185:1421-1428.
- 463 DiPietro JA, Hilton SC, Hawkins M, Costigan KA, Pressman EK (2002) Maternal stress and  
464 affect influence fetal neurobehavioral development. *Dev Psychol* 38:659-668.
- 465 DiPietro JA, Bornstein MH, Hahn CS, Costigan K, Achy-Brou A (2007) Fetal heart rate and  
466 variability: stability and prediction to developmental outcomes in early childhood. *Child*  
467 *Dev* 78:1788-1798.

468 DiPietro JA, Voegtline KM, Costigan KA, Aguirre F, Kivlighan K, Chen P (2013) Physiological  
469 reactivity of pregnant women to evoked fetal startle. *J Psychosom Res* 75:321-326.

470 DiPietro JA, Caulfield L, Costigan KA, Merialdi M, Nguyen RH, Zavaleta N, Gurewitsch ED  
471 (2004) Fetal neurobehavioral development: a tale of two cities. *Dev Psychol* 40:445-456.

472 Doria V, Beckmann CF, Arichi T, Merchant N, Groppo M, Turkheimer FE, Counsell SJ,  
473 Murgasova M, Aljabar P, Nunes RG, Larkman DJ, Rees G, Edwards AD (2010)  
474 Emergence of resting state networks in the preterm human brain. *Proc Natl Acad Sci U*  
475 *S A* 107:20015-20020.

476 Doyle C, Werner E, Feng T, Lee S, Altemus M, Isler JR, Monk C (2015) Pregnancy distress  
477 gets under fetal skin: Maternal ambulatory assessment & sex differences in prenatal  
478 development. *Dev Psychobiol* 57:607-625.

479 Fanselow MS, Dong HW (2010) Are the dorsal and ventral hippocampus functionally distinct  
480 structures? *Neuron* 65:7-19.

481 Feldman R (2006) From biological rhythms to social rhythms: Physiological precursors of  
482 mother-infant synchrony. *Dev Psychol* 42:175-188.

483 Gao W, Lin W, Grewen K, Gilmore JH (2017) Functional Connectivity of the Infant Human Brain:  
484 Plastic and Modifiable. *Neuroscientist* 23:169-184.

485 Gao W, Alcauter S, Smith JK, Gilmore JH, Lin W (2015) Development of human brain cortical  
486 network architecture during infancy. *Brain Struct Funct* 220:1173-1186.

487 Ghio M, Cara C, Tettamanti M (2021) The prenatal brain readiness for speech processing: A  
488 review on foetal development of auditory and primordial language networks. *Neurosci*  
489 *Biobehav Rev* 128:709-719.

490 Heuser CC (2020) Physiology of Fetal Heart Rate Monitoring. *Clin Obstet Gynecol* 63:607-615.

491 Hofmeyr F, Groenewald CA, Nel DG, Myers MM, Fifer WP, Signore C, Hankins GD, Odendaal  
492 HJ, Network P (2014) Fetal heart rate patterns at 20 to 24 weeks gestation as recorded  
493 by fetal electrocardiography. *J Matern Fetal Neonatal Med* 27:714-718.

494 Horiuchi J, McDowall LM, Dampney RA (2006) Differential control of cardiac and sympathetic  
495 vasomotor activity from the dorsomedial hypothalamus. *Clin Exp Pharmacol Physiol*  
496 33:1265-1268.

497 Howland MA, Sandman CA, Davis EP, Glynn LM (2020) Prenatal maternal psychological  
498 distress and fetal developmental trajectories: associations with infant temperament. *Dev*  
499 *Psychopathol* 32:1685-1695.

500 Jongen GJLM, van der Hout-van der Jagt MB, Oei SG, van de Vosse FN, Bovendeerd PHM  
501 (2017) Simulation of fetal heart rate variability with a mathematical model. *Med Eng*  
502 *Phys* 42:55-64.

503 Joshi A, Scheinost D, Okuda H, Belhachemi D, Murphy I, Staib LH, Papademetris X (2011)  
504 Unified framework for development, deployment and robust testing of neuroimaging  
505 algorithms. *Neuroinformatics* 9:69-84.

506 Karmakar C, Kimura Y, Palaniswami M, Khandoker A (2015) Analysis of fetal heart rate  
507 asymmetry before and after 35 weeks of gestation. *Biomedical Signal Processing and*  
508 *Control* 21:43-48.

509 Korom M, Camacho MC, Filippi CA, Licandro R, Moore LA, Dufford A, Zöllei L, Graham AM,  
510 Spann M, Howell B, Shultz S, Scheinost D, FIT'NG (2021) Dear reviewers: Responses  
511 to common reviewer critiques about infant neuroimaging studies. *Dev Cogn Neurosci*  
512 53:101055.

513 Koziol LF, Budding D, Andreasen N, D'Arrigo S, Bulgheroni S, Imamizu H, Ito M, Manto M,  
514 Marvel C, Parker K, Pezzulo G, Ramnani N, Riva D, Schmahmann J, Vandervert L,  
515 Yamazaki T (2014) Consensus paper: the cerebellum's role in movement and cognition.  
516 *Cerebellum* 13:151-177.

517 Kropf E, Syan SK, Minuzzi L, Frey BN (2019) From anatomy to function: the role of the  
518 somatosensory cortex in emotional regulation. *Braz J Psychiatry* 41:261-269.

519 Kumral D, Schaare HL, Beyer F, Reinelt J, Uhlig M, Liem F, Lampe L, Babayan A, Reiter A,  
520 Erbey M, Roebbig J, Loeffler M, Schroeter ML, Husser D, Witte AV, Villringer A, Gaebler  
521 M (2019) The age-dependent relationship between resting heart rate variability and  
522 functional brain connectivity. *Neuroimage* 185:521-533.

523 Kwon SH, Scheinost D, Lacadie C, Benjamin J, Myers EH, Qiu M, Schneider KC, Rothman DL,  
524 Constable RT, Ment LR (2014) GABA, Resting-State Connectivity and the Developing  
525 Brain. *Neonatology* 106:149-155.

526 Macey PM, Ogren JA, Kumar R, Harper RM (2015) Functional Imaging of Autonomic  
527 Regulation: Methods and Key Findings. *Front Neurosci* 9:513.

528 Matusik PS, Zhong C, Matusik PT, Alomar O, Stein PK (2023) Neuroimaging Studies of the  
529 Neural Correlates of Heart Rate Variability: A Systematic Review. *J Clin Med* 12.

530 Monk C, Fifer WP, Myers MM, Sloan RP, Trien L, Hurtado A (2000) Maternal stress responses  
531 and anxiety during pregnancy: effects on fetal heart rate. *Dev Psychobiol* 36:67-77.

532 Monk C, Sloan RP, Myers MM, Ellman L, Werner E, Jeon J, Tager F, Fifer WP (2004) Fetal  
533 heart rate reactivity differs by women's psychiatric status: an early marker for  
534 developmental risk? *J Am Acad Child Adolesc Psychiatry* 43:283-290.

535 Mulkey SB, Plessis AD (2018) The Critical Role of the Central Autonomic Nervous System in  
536 Fetal-Neonatal Transition. *Semin Pediatr Neurol* 28:29-37.

537 Noble S, Spann MN, Tokoglu F, Shen X, Constable RT, Scheinost D (2017) Influences on the  
538 Test-Retest Reliability of Functional Connectivity MRI and its Relationship with  
539 Behavioral Utility. *Cerebral Cortex* 27:5415-5429.

540 Oliveira V, von Rosenberg W, Montaldo P, Adjei T, Mendoza J, Shivamurthappa V, Mandic D,  
541 Thayyil S (2019) Early Postnatal Heart Rate Variability in Healthy Newborn Infants. *Front*  
542 *Physiol* 10:922.

543 Pingeton BC, Goodman SH, Monk C (2021) Prenatal origins of temperament: Fetal cardiac  
544 development & infant surgency, negative affectivity, and regulation/orienting. *Infant*  
545 *Behav Dev* 65:101643.

546 Pipe JG (1999) Motion correction with PROPELLER MRI: application to head motion and free-  
547 breathing cardiac imaging. *Magnetic Resonance in Medicine: An Official Journal of the*  
548 *International Society for Magnetic Resonance* 42:963-969.

549 Potegal M (2012) Temporal and frontal lobe initiation and regulation of the top-down escalation  
550 of anger and aggression. *Behav Brain Res* 231:386-395.

551 Robinson BF, Epstein SE, Beiser GD, Braunwald E (1966) Control of heart rate by the  
552 autonomic nervous system. Studies in man on the interrelation between baroreceptor  
553 mechanisms and exercise. *Circ Res* 19:400-411.

554 Scheinost D, Spann MN, McDonough L, Peterson BS, Monk C (2020) Associations between  
555 different dimensions of prenatal distress, neonatal hippocampal connectivity, and infant  
556 memory. *Neuropsychopharmacology* 45:1272-1279.

557 Scheinost D, Chang J, Lacadie C, Brennan-Wydra E, Constable RT, Chawarska K, Ment LR  
558 (2022) Functional connectivity for the language network in the developing brain:  
559 30 weeks of gestation to 30 months of age. *Cereb Cortex* 32:3289-3301.

560 Scheinost D, Kwon SH, Lacadie C, Vohr BR, Schneider KC, Papademetris X, Constable RT,  
561 Ment LR (2017) Alterations in Anatomical Covariance in the Prematurely Born. *Cerebral*  
562 *Cortex* 27:534-543.

563 Spann M, Smerling J, Gustafsson HC, Foss S, Monk C (2014) Fetal Neurobehavioral  
564 Development and the Role of Maternal Nutrient Intake and Psychological Health. *Zero to*  
565 *Three* 34.

566 Spann MN, Monk C, Scheinost D, Peterson BS (2018) Maternal Immune Activation During the  
567 Third Trimester Is Associated with Neonatal Functional Connectivity of the Salience  
568 Network and Fetal to Toddler Behavior. *J Neurosci* 38:2877-2886.

569 Spann MN, Smerling J, Gustafsson H, Foss S, Altemus M, Monk C (2015) Deficient maternal  
570 zinc intake-but not folate-is associated with lower fetal heart rate variability. *Early Hum*  
571 *Dev* 91:169-172.

572 Steiger JH (1980) Tests for comparing elements of a correlation matrix. *Psychological Bulletin*  
573 87:245-251.

574 Sun H, Jiang R, Dai W, Dufford AJ, Noble S, Spann MN, Gu S, Scheinost D (2023) Network  
575 controllability of structural connectomes in the neonatal brain. *Nat Commun* 14:5820.

576 Suwanrath C, Suntharasaj T (2010) Sleep-wake cycles in normal fetuses. *Arch Gynecol Obstet*  
577 281:449-454.

578 Szucs D, Ioannidis JP (2020) Sample size evolution in neuroimaging research: An evaluation of  
579 highly-cited studies (1990-2012) and of latest practices (2017-2018) in high-impact  
580 journals. *Neuroimage* 221:117164.

581 Thomason ME, Grove LE, Lozon TA, Vila AM, Ye Y, Nye MJ, Manning JH, Pappas A,  
582 Hernandez-Andrade E, Yeo L, Mody S, Berman S, Hassan SS, Romero R (2015) Age-  
583 related increases in long-range connectivity in fetal functional neural connectivity  
584 networks in utero. *Dev Cogn Neurosci* 11:96-104.

585 Thompson BL, Levitt P (2010) The clinical-basic interface in defining pathogenesis in disorders  
586 of neurodevelopmental origin. *Neuron* 67:702-712.

587 Ulrich-Lai YM, Herman JP (2009) Neural regulation of endocrine and autonomic stress  
588 responses. *Nat Rev Neurosci* 10:397-409.

589 Van Dijk KR, Sabuncu MR, Buckner RL (2012) The influence of head motion on intrinsic  
590 functional connectivity MRI. *Neuroimage* 59:431-438.

591 Werner EA, Myers MM, Fifer WP, Cheng B, Fang Y, Allen R, Monk C (2007) Prenatal predictors  
592 of infant temperament. *Dev Psychobiol* 49:474-484.

593 Williams JHG, Huggins CF, Zupan B, Willis M, Van Rheenen TE, Sato W, Palermo R, Ortner C,  
594 Krippel M, Kret M, Dickson JM, Li CR, Lowe L (2020) A sensorimotor control framework  
595 for understanding emotional communication and regulation. *Neurosci Biobehav Rev*  
596 112:503-518.

597 Wong C, Gallate J (2012) The function of the anterior temporal lobe: a review of the empirical  
598 evidence. *Brain Res* 1449:94-116.

599 Zisser H, Jovanovic L, Thorsell A, Kupperman A, Taylor LJ, Ospina P, Hod M (2006) The fidgety  
600 fetus hypothesis: fetal activity is an additional variable in determining birth weight of  
601 offspring of women with diabetes. *Diabetes Care* 29:63-67.

602

603

604

605 **Table 1.** Results of the correlations between bilateral medulla, hypothalamus, and  
 606 dACC voxel-wise neonate functional connectivity and third trimester mean resting fetal  
 607 HR and HRV (n=48).

Seed (bilateral)	Region	Volume (# voxels)	Association type
<b>FETAL MEAN HEART RATE</b>			
<b>MEDULLA</b>			
	Pre/postcentral gyrus (L)	496	Positive
	Pre/postcentral gyrus (R+L)	339	Positive
	Inferior parietal lobe (R)	239	Positive
<b>HYPOTHALAMUS</b>			
	Middle frontal gyrus (L)	327	Positive
	Middle frontal gyrus (R)	284	Positive
<b>dACC</b>			
	Cerebellum (L)	480	Negative
	Inferior parietal lobule & Superior temporal gyrus (L)	273	Positive
<b>FETAL MEAN HEART RATE VARIABILITY</b>			
<b>MEDULLA</b>			
	Precuneus & paracentral lobule (L)	331	Positive
<b>HYPOTHALAMUS</b>			
	Middle temporal gyrus (L)	323	Negative
<b>dACC</b>			
	Lateral occipital gyrus (R)	412	Positive
	Superior frontal gyrus (L)	328	Positive

608

609

610

611



612 **Table 2.** Results of the correlations between bilateral medulla, hypothalamus and dACC  
 613 voxel-wise neonate functional connectivity and second trimester mean resting fetal HR  
 614 and HRV (n=33).

615

Seed (bilateral)	Region	Volume (# voxels)	Association type
<b>FETAL MEAN HEART RATE</b>			
<b>MEDULLA</b>			
	Middle frontal gyrus (L)	437	Negative
	Superior temporal gyrus & inferior parietal lobule (R)	317	Positive
<b>HYPOTHALAMUS</b>			
	Subcortex (L)	324	Positive
	Precuneus & paracentral lobule (L)	215	Positive
<b>dACC</b>			
	Insula (L)	587	Negative
	Cerebellum lobules V-VI & Crus I (R)	567	Negative
	Visual cortex (R-L)	382	Positive
	Lateral occipital gyrus (R)	251	Positive
	Basal ganglia (R)	226	Negative
<b>FETAL HEART RATE VARIABILITY</b>			
<b>MEDULLA</b>			
	Cerebellum lobules V-VI & fusiform gyrus (L)	964	Positive
	Cerebellum lobules V-VI (R)	208	Positive
	Superior parietal lobule (R)	204	Positive
<b>HYPOTHALAMUS</b>			
	Subcortex (R)	768	Positive
	Subcortex (L)	320	Positive
<b>dACC</b>			
	Middle cingulate cortex	226	Negative

617

618

619

620

621

622 **Table 3.** Results of the correlations between bilateral medulla, hypothalamus, and  
 623 dACC neonate functional connectivity and the change from second to third trimester  
 624 mean resting fetal HR and HRV (n=27).

625

626

Seed (bilateral)	Region	Volume (# voxels)	Association type
<b>CHANGE IN FETAL MEAN HEART RATE</b>			
<b>MEDULLA</b>			
	Pre/postcentral gyrus (L)	1144	Positive
	Cerebellum (R+L)	1043	Negative
<b>dACC</b>			
	Inferior frontal gyrus (R)	376	Positive
<b>CHANGE IN FETAL HEART RATE VARIABILITY</b>			
<b>MEDULLA</b>			
	Cerebellum (R)	379	Negative
	Hippocampus (L)	337	Negative
	Inferior occipital gyrus (R)	203	Positive
<b>HYPOTHALAMUS</b>			
	Precentral gyrus (L)	418	Positive
	Precuneus and paracentral lobule (R)	267	Positive
	Middle temporal gyrus (L)	256	Negative
	Precuneus and paracentral lobule (L)	218	Positive
<b>dACC</b>			
	Middle frontal gyrus (L)	480	Positive

627

628

629

630 **Figure 1.** Sagittal views of the three regions of interest used for seed analysis that were  
631 manually defined on a custom, neonatal template (Spann et al., 2018). The bilateral medulla is  
632 shown in blue. The hypothalamus is shown in green. The dorsal anterior cingulate cortex  
633 (dACC) is shown in red. The approximate MNI coordinates are: dACC (-1,24,26), medulla (-4, -  
634 36,-35), and hypothalamus (-2,-3,-3). The temporal signal noise ratios for each seed are  
635  $49.37 \pm 32.84$  for the medulla,  $65.36 \pm 34.86$  for the hypothalamus, and  $170.71 \pm 109.35$  for the  
636 dACC.

637

638

639

JNeurosci Accepted Manuscript

640 **Figure 2. Associations between mean fetal heart rate (HR) during in the third trimester and**  
641 **newborn bilateral medulla, hypothalamus and dACC connectivity (n=48).** (*top*) Higher mean  
642 fetal HR was positively associated with newborn connectivity between bilateral medulla and  
643 bilateral precentral, postcentral gyrus and the right inferior parietal lobe. (*middle*) Higher levels of  
644 mean fetal HR were positively associated with newborn connectivity between bilateral  
645 hypothalamus and the left and right middle frontal gyrus (left panel). (*bottom*) Higher levels of  
646 mean fetal HR were negatively associated with newborn connectivity between bilateral dACC and  
647 the left cerebellum. Higher levels of mean fetal HR positively associated with bilateral dACC and  
648 left inferior parietal lobule and superior temporal gyrus connectivity.

649

650

651

652

653

654

655

656

657

658 **Figure 3. Associations between fetal heart rate variability (HRV) during in the third**  
659 **trimester and newborn bilateral medulla, hypothalamus, and dACC connectivity (n=48).**  
660 (*top*) Higher fetal HRV was positively associated with the connectivity between the medulla and  
661 the left precuneus and paracentral lobule. (*middle*) Higher fetal HRV was inversely associated  
662 with the connectivity between the hypothalamus and the left middle temporal gyrus. (*bottom*)  
663 Higher fetal HRV was positively associated with connectivity between the bilateral dACC and the  
664 left superior frontal gyrus and between the bilateral dACC and the right lateral occipital gyrus.  
665

JNeurosci Accepted Manuscript

666

667 **Figure 4. Associations between the mean fetal HR during in the second trimester and**  
668 **newborn bilateral medulla, hypothalamus and dACC connectivity (n=33).** (*top*) Higher mean  
669 fetal HR was inversely associated with the medulla-left MFG connectivity and positively with  
670 medulla-right STG and IPL connectivity. (*middle*) Higher mean fetal HR was positively associated  
671 with the connectivity between the hypothalamus and left subcortex and between the  
672 hypothalamus and left precuneus/paracentral lobule. (*bottom*) Higher mean fetal HR was  
673 inversely associated with the connectivity between the dACC and the right cerebellum, between  
674 the dACC and the right basal ganglia, and between the dACC and left insula. Higher mean fetal  
675 HR was associated with the connectivity between the dACC and the bilateral visual cortex and  
676 between the dACC and the right lateral occipital gyrus.

677

678

JNeurosci Accepted Manuscript

679 **Figure 5. Associations between fetal HRV during in the second trimester and newborn**  
680 **bilateral medulla, hypothalamus, and dACC connectivity (n=33).** *(top)* Higher fetal HRV was  
681 positively associated with the connectivity between the medulla and right cerebellum, between  
682 the medulla and the left fusiform gyrus/cerebellum, and between the medulla and right SPL.  
683 *(middle)* Higher fetal HRV was positively associated with connectivity between hypothalamus and  
684 right and left subcortex. *(bottom)* Higher fetal HRV was positively associated with connectivity  
685 between dACC and middle cingulate cortex.

686

JNeurosci Accepted Manuscript

687 **Figure 6. Associations of the change in mean fetal HR from the second to third trimester**  
688 **with bilateral medulla, hypothalamic, and dACC connectivity in neonates (n=27).** *(top)*  
689 Higher change in fetal HR was positively associated with the connectivity between the medulla  
690 and the left precentral and postcentral gyrus and inversely associated with the connectivity  
691 between the medulla and the cerebellum. *(bottom)* Higher change in fetal HR was positively  
692 associated with the connectivity between the dACC and the right inferior frontal gyrus.

693

694

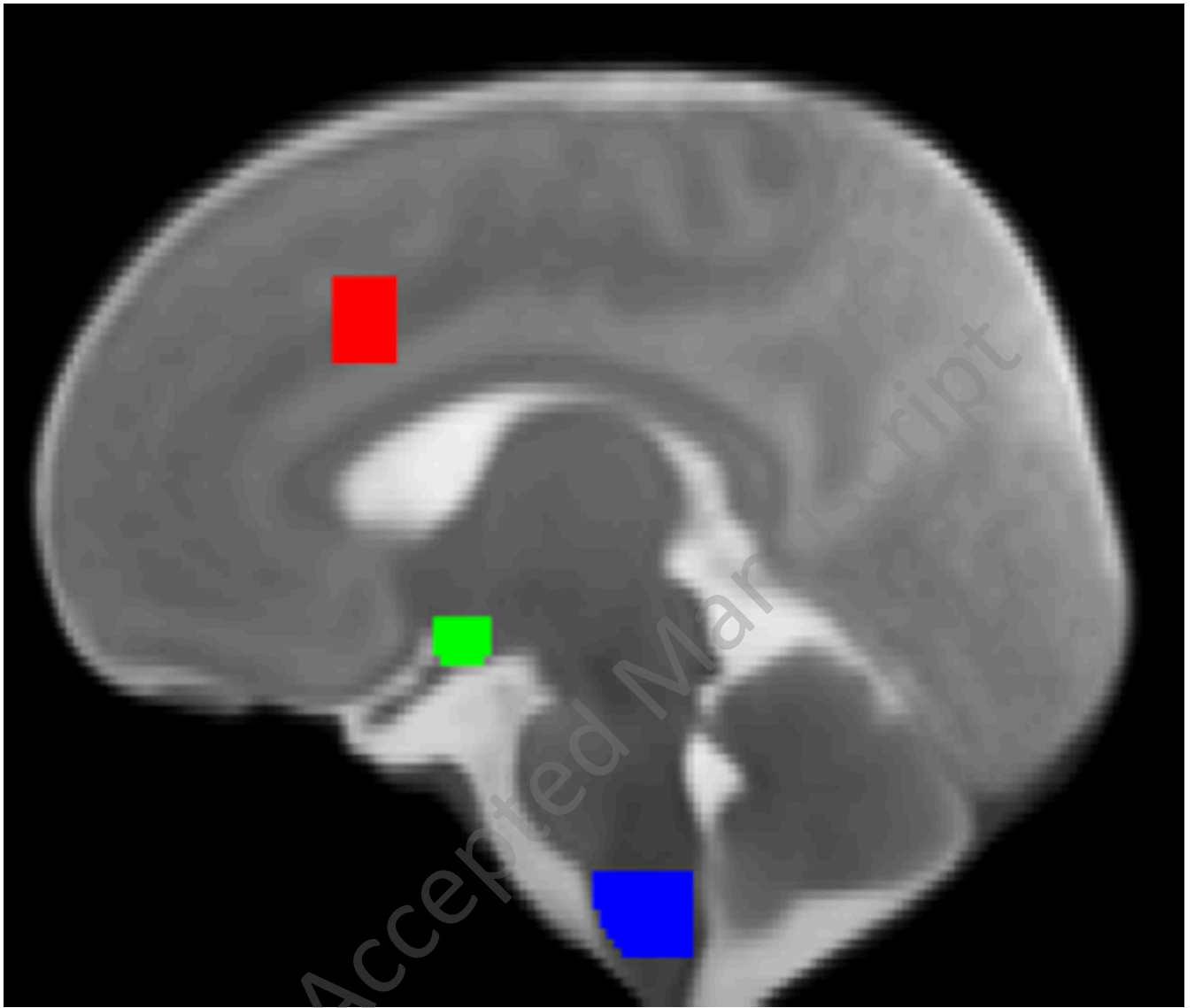
695

696

JNeurosci Accepted Manuscript



697 **Figure 7. Associations of the change in fetal HRV from the second to third trimester with**  
698 **bilateral medulla, hypothalamic, and dACC connectivity in neonates (n=27).** *(top)* Higher  
699 change in fetal HRV was positively associated with the connectivity between the medulla and the  
700 right inferior occipital gyrus and was inversely associated with the connectivity between the  
701 medulla and the left hippocampus and between the medulla and right cerebellum. *(middle)* Higher  
702 change in fetal HRV was positively associated with the connectivity between the hypothalamus  
703 and the bilateral precuneus and paracentral lobule and between the hypothalamus and the left  
704 precentral gyrus. Higher change in fetal HRV was inversely associated with the connectivity  
705 between the hypothalamus and middle temporal gyrus. *(bottom)* Higher change in fetal HRV was  
706 positively associated with the connectivity between the dACC and the left middle frontal gyrus.  
707



JNeurosci Accepted Manuscript

